Indazoles in Drug Discovery

Key Points

- A good bioisostere for phenol

- A privileged fragment in FBDD

- A privileged scaffold in scaffold hopping exercises, especially for protein kinase inhibitors

Overview

Indazole is important in at least three major areas in medicinal chemistry. a. It is a good bioisostere for phenol. Generally speaking, phenol's heterocyclic bioisosteres, including indazoles, tend to be more lipophilic and less vulnerable to phase I and II metabolism in comparison to phenol itself. b. Indazole is a privileged fragment in FBDD. c. It has proven to be a privileged scaffold in scaffold hopping exercises, especially for protein kinase inhibitors.

PharmaBlock

Indazole has two isomers: 1*H*-indazole and 2*H*-indazole. Both of them may potentially serve as bioisosteres for indole. Like indole, indazole has an NH group to serve as a hydrogen bond donor. Unlike indole, indazole has an additional nitrogen atom to serve as a hydrogen bond acceptor. This may provide improved affinity to the target protein. Indazole is a privileged scaffold for many kinase inhibitors, presumably forming pivotal interactions with hinge residues.

indole   1*H*-indazole   2*H*-indazole

Indazole is important in at least three major areas in medicinal chemistry. a. Indazole is a good bioisostere for phenol. Generally speaking, phenol's heterocyclic bioisosteres, including indazole, tend to be more lipophilic and less vulnerable to phase I and II metabolism in comparison to phenol. b. Indazole is a privileged fragment in fragment-based drug discovery (FBDD). c. Indazole has proven to be a privileged scaffold in scaffold hopping exercises, especially for protein kinase inhibitors.

Indazole-containing Drugs

There are about six indazole-containing drugs on the market. Several aza-indazole-containing drugs have also gained regulatory approval. 1*H*-Indazole bendazac (**1**) is an old non-steroidal anti-inflammatory drug (NSAID). Bendazac (**1**) and its main metabolite, the 5-hydroxyl derivative, provide antioxidant effects as scavengers of oxygen-derived free radicals. Bendazac lysine salt as an anti-denaturant is nowadays used as an eye drop to treat cataracts. Benzyldamine (**2**), a bendazac (**1**) analog, is also an NSAID used for treating cataracts. The third analog, lonidamine, has only been explored at the preclinical stages. Roche's granisetron (Kytril, **3**), a serotonin 5-HT$_3$ receptor antagonist used as an antiemetic to treat nausea and vomiting following chemotherapy, has a 1*H*-indazole core structure. Pfizer's axitinib (Inlyta, **4**), also a 1*H*-indazole, is a dual vascular endothelial growth factor receptor (VEGFR) and platelet-derived growth factor receptor (PDGFR) inhibitor.

GSK's pazopanib (Votrient, **5**), a 2*H*-indazole, is a VEGFR and c-Kit inhibitor. Tesaro's poly(ADP-ribosyl) polymerase (PARP) inhibitor niraparib (Zejula, **6**) is also a 2*H*-indazole
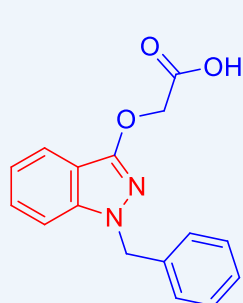
bendazac (**1**)
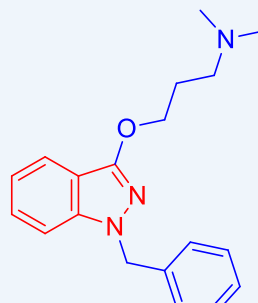
benzyldamine (**2**)
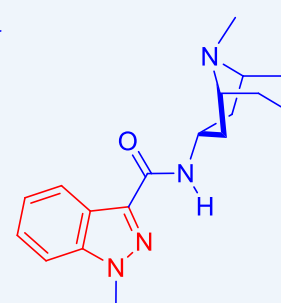
granisetron (Kytril, **3**)
Beecham/Roche, 1994
5-HT$_3$ receptor antagonist
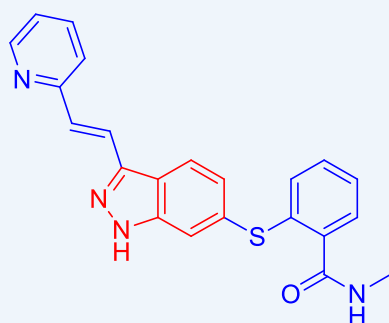
axitinib (Inlyta, **4**)
Pfizer, 2012
VEGF and PDGFR inhibitor
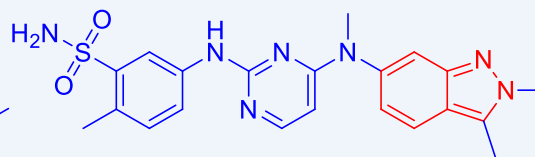
pazopanib (Votrient, **5**)
GSK, 2009
VEGFR, c-Kit inhibitor
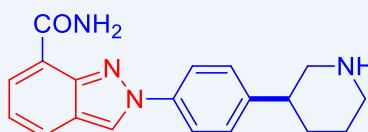
niraparib (Zejula, **6**)
Tesaro, 2017
PARP inhibitor

Indazoles in Drug Discovery

Indazole has been used in at least three major areas in drug discovery: (a) as the biostere for phenol and indole, (b) as a fragment for fragment-based drug discovery (FBDD) in drug discovery, and (c) as a scaffold in scaffold hopping.

a. Indazole as a bioisostere of phenol

Back in the 1980s, Schering–Plough reported the discovery of the first high-affinity and selective D_1/D_5 antagonist SCH 23390 (**7**). However, benzazepine **7** was inactive in rhesus monkeys with a very short duration of action. Pharmacokinetic (PK) evaluation revealed that extensive *O*-glucuronidation of the phenol and *N*-dealkylation of the N–Me group *in vivo* may have contributed to its poor PK profile. Schering–Plough chose to replace the metabolically problematic phenol with indazole and other heterocycles with hydrogen bond donating NH functionality. *Generally speaking, phenol's heterocyclic bioisosteres tend to be more lipophilic and less vulnerable to phase I and II metabolism in comparison to phenol itself.* Indeed, indazole analog **8** began to show improved PK profile although it was tested about ten-fold less potent than SCH 23390 (**7**). As a testimony to the importance of the hydrogen bond donating NH functionality, methylated indazole **9** had significantly decreased (6x) affinity for the D_1 receptor.[1]

SCH 23390 (**7**)
D_1 K_i = 1.4 nM
D_5 K_i = 2.8 nM
rat PK (10 mg/kg, po)
AUC = 0 h•μg/mL
C_{max} = 0 ng/mL
T_{max} = 0 h

indazole **8**
D_1 K_i = 14 nM
D_5 K_i = 30 nM
rat PK (10 mg/kg, po)
AUC = 0.06 h•μg/mL
C_{max} = 15 ng/mL
T_{max} = 2 h

methylated indazole **9**
D_1 K_i = 183 nM

PharmaBlock Products

MeOOC

Cl

PBLJ3576

Br

MeO
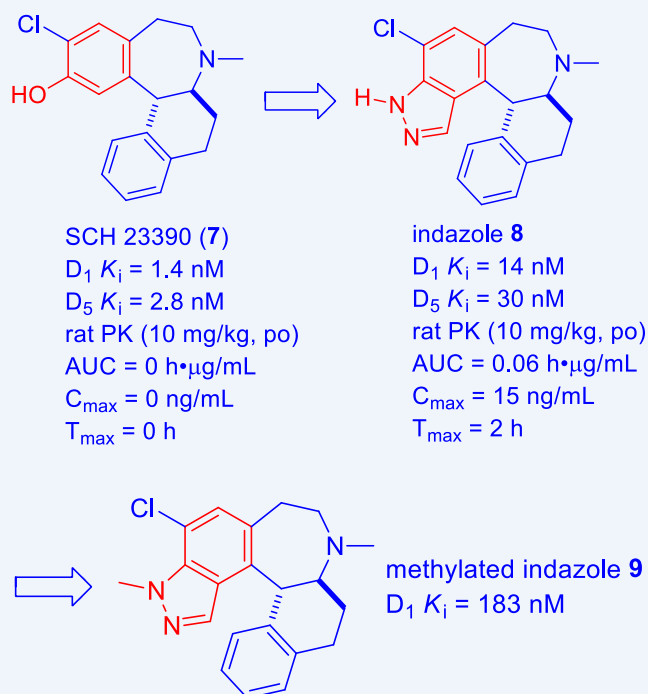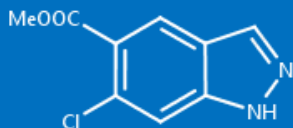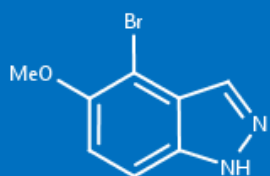
PBGJ2055

Lymphocyte-specific protein tyrosine kinase (Lck) is a member of the Src family of tyrosine kinases and Lck inhibitors may offer an approach to treat T cell-mediated inflammatory disorders. One of GSK's Lck inhibitors, phenol **10**, was potent with an IC_{50} value of 8.5 nM in an Lck biochemical assay. In the docking model, the oxygen of phenol **10**'s 5-hydroxyl group is 2.3 Å away from the backbone NH of Lck's Asp_{382}, indicating that the oxygen here serves as a hydrogen bond acceptor. Meanwhile, the phenol's hydrogen is 2.7 Å away from the side-chain of Glu_{288}, implying that either Glu_{288} moves closer when the compound binds or that a water-mediated interaction is present. Unfortunately, phenol **10** has a poor pharmacokinetic profile, exhibiting high clearance, short half-life, and low oral bioavailability. This is not all that surprising since phenols are prone to phase I and II metabolism.[2]

Indazole as an isostere for phenol again proved to be fruitful here and phenol **10**'s indazole analog **11** was tested potent with an improved protein kinase selectivity profile. Docking modeling indicated that their hydrogen bonding vectors mimic each other very closely, maintaining the direct interaction with Asp_{382} and the direct or water-mediated hydrogen bond to Glu_{288}. More importantly, indazole **11** demonstrated superior PK profile for both IV and p.o. routes of administration with a 25% oral bioavailability, (*F* %), whereas the value for phenol **10** was 0%.[2]

Phosphatidylinositol 3-kinases (PI3K) play a central role in a broad cellular functions including cell growth, proliferation, differentiation, survival, and intracellular trafficking. Gilead's PI3Kδ selective inhibitor idelalisib (Zydelig) was approved in 2014 and Bayer's pan-PI3K inhibitor copanlisib (Aliqopa) in 2017.

phenol **10**
Lck IC_{50} = 8.5 nM
IV Cl_p = 65.5 mL/min/kg
IV V_{ss} = 0.3 L/kg
IV $T_{1/2}$ = 0.12 h
IV AUC_{0-t} = 635 ng•h/mL
mouse p.o., F % < 1%

Glu288
Lck
Asp382

indazole **11**
Lck IC_{50} = 19 nM
IV Cl_p = 22.4 mL/min/kg
IV V_{ss} = 0.7 L/kg
IV $T_{1/2}$ = 0.53 h
IV AUC_{0-t} = 743 ng•h/mL
mouse p.o., F % = 25%
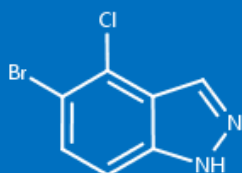
Glu288
Lck
Asp382
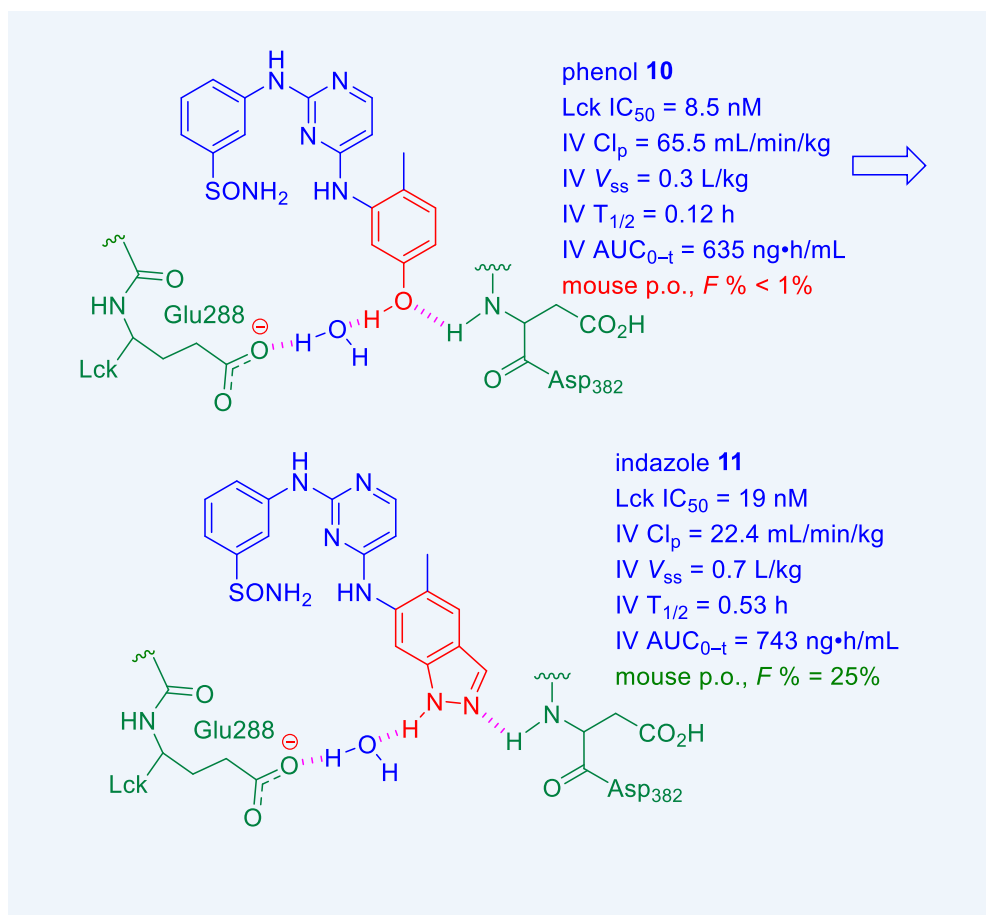
Using Hayakawa's 4-morpholino-2-phenylquinazoline PI3Kα p110$\alpha\alpha$ inhibitors as a starting point,[3a] Genentech arrived at phenol **12**. But its bioavailability was low in mouse and rat, even though it displayed enhanced metabolic stability in human and mouse microsomes. Again, this is mainly due to O-glucuronidation of the phenol group. The metabolic liability was addressed once again by employing the indazole isostere. At the end, indazole **13** (GDC-0941, pictilisib) was not only potent and selective for PI3Kα over PI3Kβ, δ, and γ subtypes, but also exhibited acceptable oral bioavailability in all species tested. The crystal structure of **13** bound to p110α revealed that the two nitrogen atoms on indazole are in hydrogen bonding distance to the phenol oxygen of Tyr867 and the carbonyl group of Asp841. Pictilisib (**13**) was advanced to phase I and II clinical trials but is no longer progressing at the moment.[3b]

PharmaBlock Products

PBZS0027

PBTQ8157

phenol **12**
PI3Kα IC$_{50}$ = 10 nM
metabolic stability in
human and mouse
microsomes = 85–90%
F % = 0–11%

GDC-0941 (pictilisib, **13**)
PI3Kα IC$_{50}$ = 3 nM
mouse   *F* % = 77%
rat   *F* % = 30%
dog   *F* % = 71%
monkey *F* % = 20%
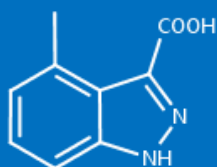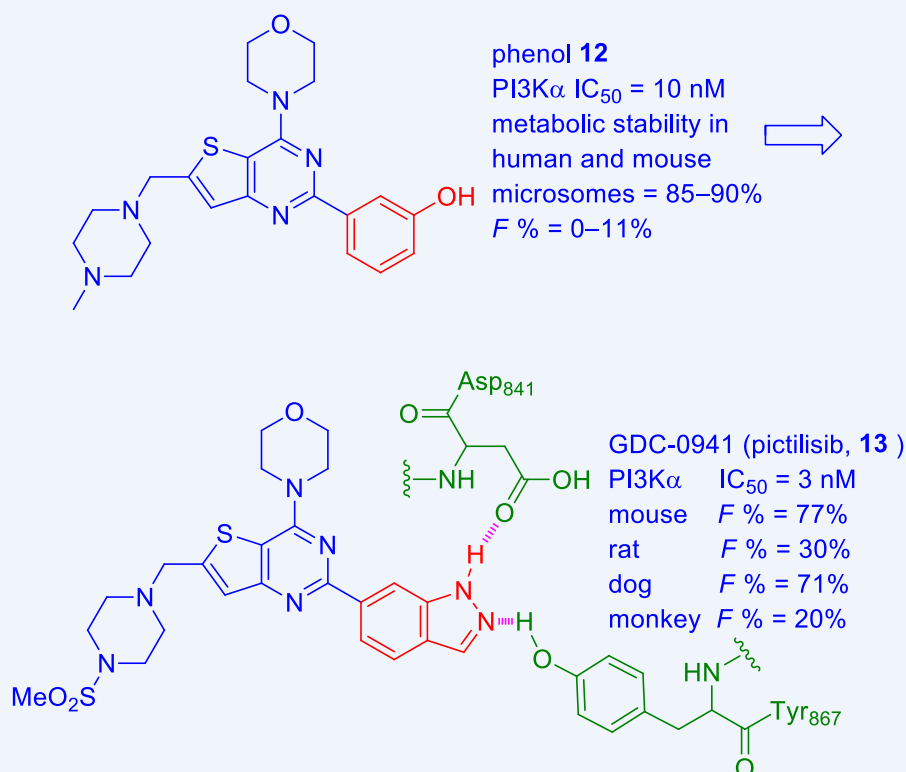
The Ras-MAP kinase pathway has been implicated in tumor progression for a variety of human cancers. The Raf kinases, which are components of this cascade, are serine/threonine kinases that activate MEK1/2. Mutant B-Raf containing a V600E substitution (where B-Raf protein's 600th amino acid valine is replaced by glutamic acid) causes aberrant constitutive activation of this pathway and has high occurrence in several human cancers. Three B-Raf kinase inhibitors have been approved by the FDA to treat cancer: vemurafenib (Zelboraf, 2011), dabrafenib (Tafinlar, 2013), and encorafenib (Braftovi), with vemurafenib (Zelboraf) being the first marketed drug that was discovered employing fragment-based drug discovery (FBDD) strategy.
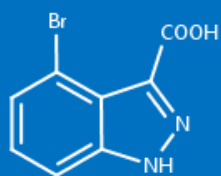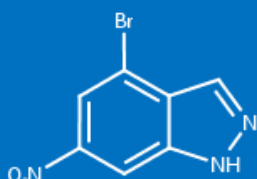
Phenol **14** is a B-raf inhibitor (IC_{50}, 0.3 nM). Bioisosterism was deployed to address the potential metabolic soft spot posed by the phenol. Although replacing the phenol functional group with hydrogen bond *acceptors*, not surprisingly, did not work (low potency), isosteric substitution with hydrogen bond *donors* offered indole **15** (IC_{50}, 36 nM) and indazole **16** (IC_{50}, 2 nM), respectively, that were active. More important, **16** potently inhibited cell proliferation at sub-micromolar concentrations in the B-Raf V600E human melanoma cell lines A375 and WM266. Subsequent docking suggested that the indazole N and NH form two hydrogen bonds with B-Raf's Glu_{501} and Asp_{594}, respectively. This exercise demonstrated again that indazole is an effective isostere for phenol.[4]

phenol **14**
B-raf, IC_{50} = 0.3 nM
A375, IC_{50} = 570 nM
WM266-4, IC_{50} = 230 nM

indole **15**
B-raf, IC_{50} = 36 nM
A375, IC_{50} = 7.5 μM
WM266-4, IC_{50} > 10 μM

indazole **16**
B-raf, IC_{50} = 2 nM
A375, IC_{50} = 380 nM
WM266-4, IC_{50} = 300 nM
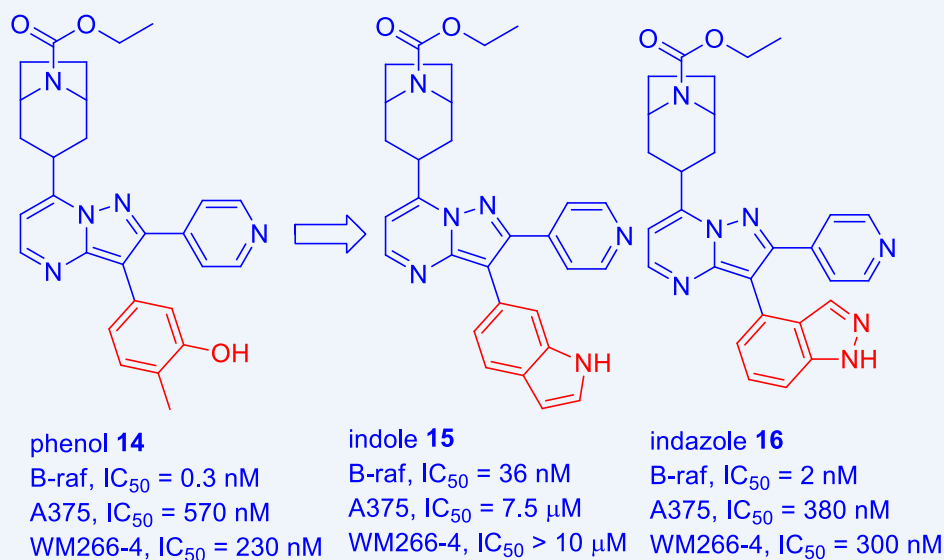
b. *Indazole as a fragment in FBDD*

In the field of kinase inhibitors, indazoles and azaindoles, among many heteroarenes, have been fruitful fragments in FBDD.

PharmaBlock Products
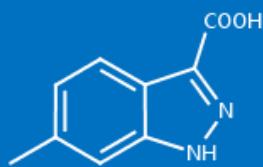
PBTQ8468
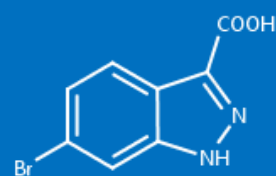
PB02053

Screening "lead-like" fragment library with an average molecular weight 160 provided fragment bromoaminoindazole **17** as a JAK-2 inhibitor with an IC_{50} value of 40.9 µM. The co-crystal structure of indazole **17** and JAK2 revealed that they make two hydrogen-bonded contacts with the hinge residues Glu_{930} and Leu_{932}, respectively. Guided by X-ray co-crystal structures, structure–activity relationship (SAR) investigations led to aminoindazole **18** with an IC_{50} value of 78 nM while maintaining a 0.41 ligand efficiency (LE = $-RTlnIC_{50}$/HAC, HAC = heavy atom count) value.[5]

bromoaminoindazole **17**
JAK-2, IC_{50} = 40.9 µM
LE = 0.54

aminoindazole **18**
JAK-2, IC_{50} = 78 nM
LE = 0.41
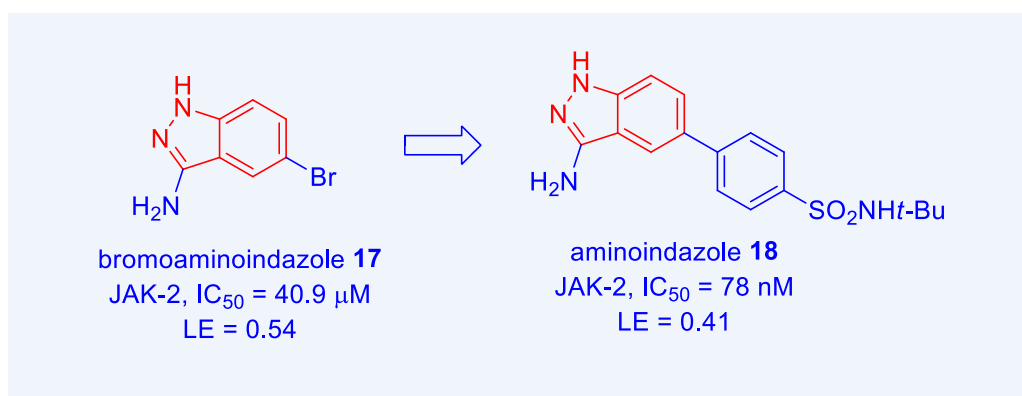
Also in the JAK arena, fragment hit **19** was obtained from screening a kinase-targeted library of 500 fragments against JAK2 at a single concentration of 100 µM. Similar to that of bromoaminoindazole **17**, the co-crystal structure of indazole **19** and JAK2 revealed that they make two hydrogen-bonded contacts with the hinge residues Glu_{930} and Leu_{932} as well. Growing fragment hit **19** by installing a phenol moiety at the 6-position afforded greatly improved potency. Fine-tuning the substituents on the phenol and sulfonamide moieties gave rise to "lead-like" indazole **20**.[6]

fragment hit **19**
JAK1 pIC_{50} = 4.5 (30 µM)
JAK2 pK_D = 4.9 (13 µM)
JAK1 LE = 0.45

lead **20**
JAK1 pIC_{50} = 8.4
cell pIC_{50} = 7.0
LE = 0.45
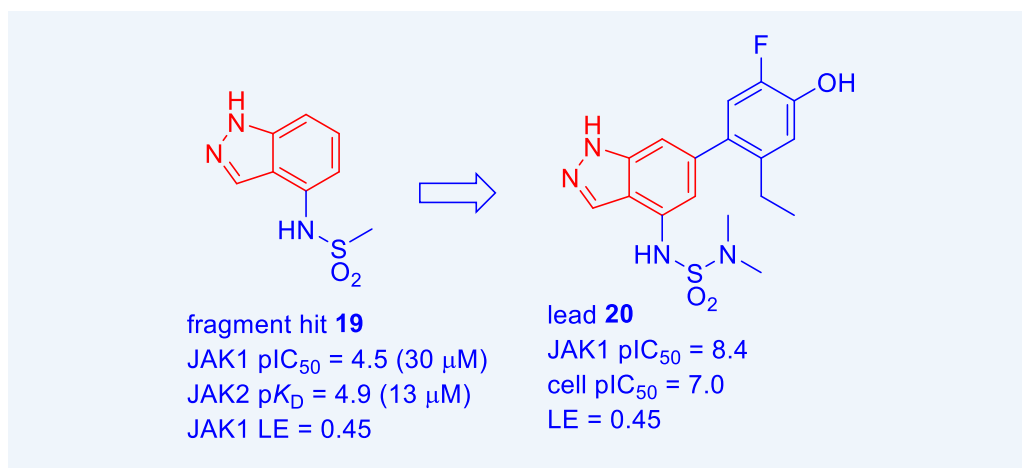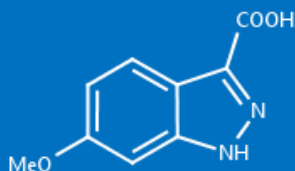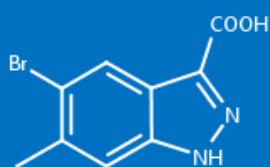
It has been observed that subtle changes in the chemistry of a fragment can induce a change in compound orientation in the crystal structure with the target protein. The crystal structure of fragment **21** and heat shock protein-90 (Hsp90) showed that they interact via hydrogen bonds of both nitrogen atoms to Asp_{93} and the conserved water molecule. Interestingly, an identical interaction pattern was found for the phenolic OH group of fragment **22**, but not its indazole NH! Similar phenomenon was observed for hydroxyindazole fragments before.[7] The reversed orientation might be influenced by the substitution pattern of the hydroxyindazole core as the cyclohexyl ring of fragment **22** is bound in the lipophilic pocket of the helical form. In contrast, this lipophilic pocket is not addressed by fragment **21**, but its phenolic substituent forms π-interactions to Met_{98} toward the solvent entrance of the ATP-site. In due course, SAR investigations via fragment elaboration/decoration led to the discovery of a series of hydroxy-indazole-carboxamides as potent Hsp90 inhibitors. Compound **23**, for example, possessed significantly improved affinity and anti-proliferative effects in different human cancer cell lines as demonstrated by cell viability assays.[8]
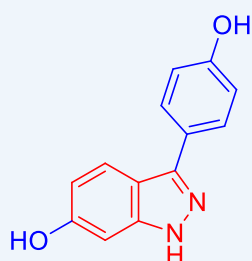
fragment **21**
MW 226
Hsp90 IC_{50} = 45 μM
LE = 0.35
BEI = 19.2
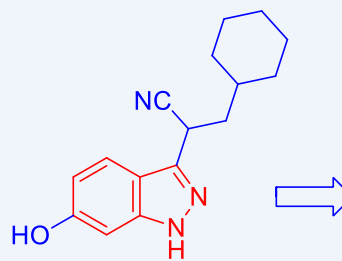
fragment **22**
MW 269
Hsp90 IC_{50} = 485 μM
LE = 0.28
BEI = 15.1
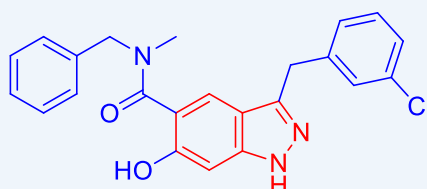
Hsp90 inhibitor **23**
Hsp90 binding assay,
IC_{50} = 60 nM
A2780 viability assay,
IC_{50} = 57 nM

Fragment **24** was obtained from an Aurora kinase A inhibition assay. Docking studies indicated that the N1-H on **24** formed hydrogen bond with the carbonyl of Glu$_{211}$, whereas the N2 atom is hydrogen bonded to the backbone of Ala$_{213}$. Subsequent *in silico* FBDD approach identified aryloyl analog **25** with the highest ligand efficiency (LE). Eventually, knowledge-based drug design provided inhibitor **26**, which had 60-fold improvement in potency over **25**. Molecular docking analysis of **26**'s binding information revealed that its indazole core forms hydrogen bonds with the hinge residues Glu$_{211}$ and Ala$_{213}$ as in the case for fragment **24**.[9]

inhibitor **24**
Aurora A IC$_{50}$ = 13 μM

inhibitor **25**
Aurora A IC$_{50}$ = 1.66 μM

inhibitor **26**
Aurora A IC$_{50}$ = 26 nM
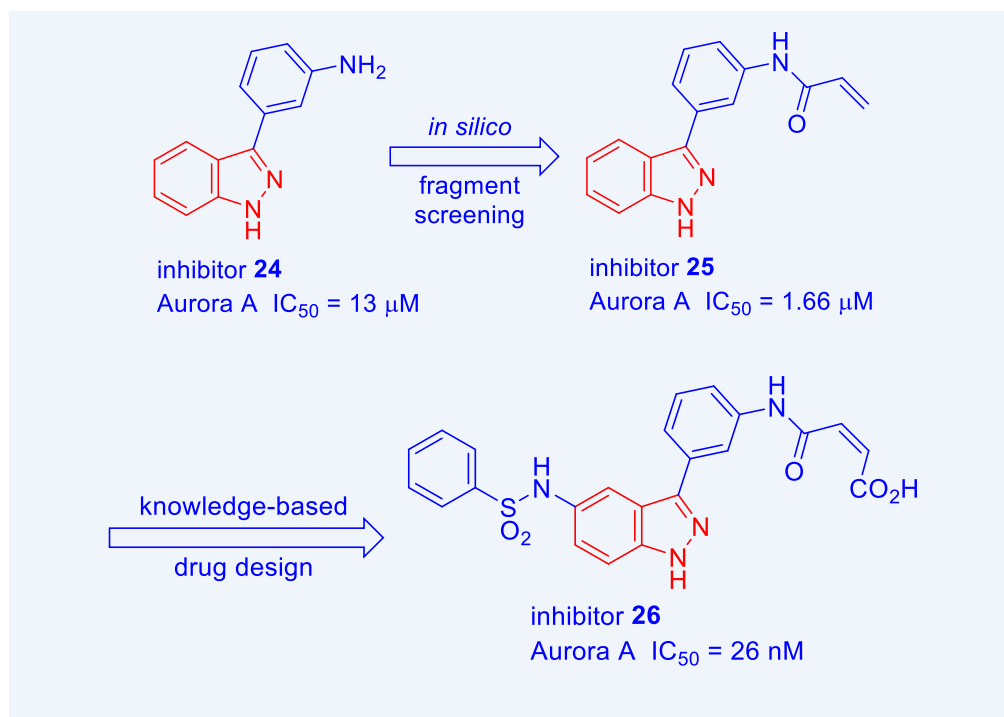
Indazole **27** was generated via an *in silico* high throuput screen (HTS) as an Unc-51-like kinase 1 (ULK1) inhibitor. Docking analysis indicated that the indazole ring system makes two hydrogen bond interactions with the amide backbone of the hinge region, specifically Glu$_{93}$ and Cys$_{95}$. Subsequent structure-guided rational drug design produced ULK1 inhibitor **28**, which had not only increased activity against ULK1, but also showed certain stability in human microsomes with negligible CYP inhibition.[10]

PharmaBlock Products

PB08302

PBLJ3246

in silico HTS hit **27**
ULK1 IC$_{50}$ = 22.4 μM

ULK1 inhibitor **28**
IC$_{50}$ = 45 nM, t$_{1/2}$ = 224 min (human)
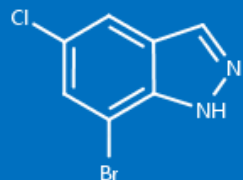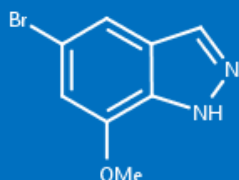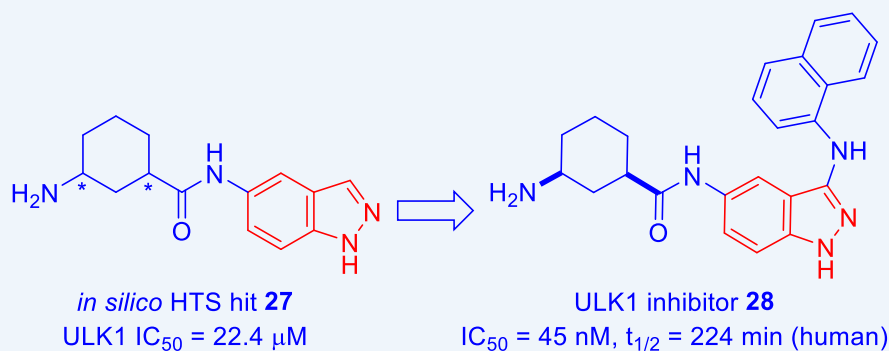
Indazole **30**, as a covalent epidermal growth factor receptor (EGFR) inhibitor was obtained employing hit compound pyrazole **29** as the starting point. It showed a strikingly increased inhibitory effect on the drug-resistant mutant of EGFR. Structurally, as a hinge-binding element, the indazole scaffold provided suitable chemical and spatial features to accommodate the space between the hinge region and the gatekeeper residues, without suffering from steric clashes with the methionine side chain. Additionally, the indazole moiety played a prominent role in forming hydrogen bonds with the peptide backbone of residues Glu$_{339}$ and Met$_{341}$. The phenyl part of the indazole furnished a favorable hydrophobic gatekeeper interaction, resulting in improved protein–ligand interactions.[11]

hit compound pyrazole **29**

indazole **30**
EGFR, IC$_{50}$ (μM)
L858R/T790M, 70 nM
L858R, 0.5 μM
wild-type, 1.7 μM
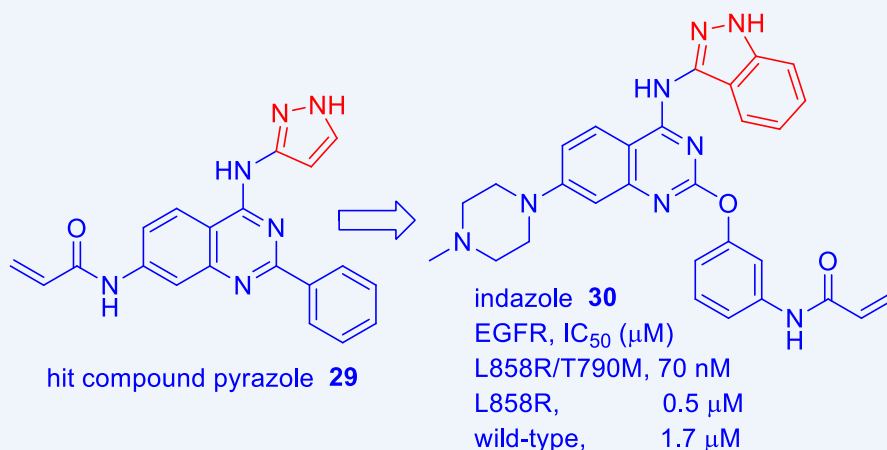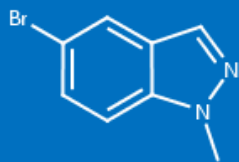
c. Indazole in scaffold hopping

At least five non-nucleoside HIV reverse transcriptase inhibitors (NNRTIs) are now on the market to combat HIV/AIDS. But HIV can become resistant to any single antiretroviral drug so combination of drugs is required. On the other hand, a single drug with features of two drugs may offer advantages against the clinically relevant mutations of reverse transcriptase, particularly K103N and Y181C. Using molecular hybridization based on crystallographic overlays of efavirenz (Sustiva, **31**) and the second-generation NNRTI capravirine **32**, a series of indazoles, as represented by **33**, were discovered as novel NNRTIs with excellent metabolic stability and mutant resilience.[12]
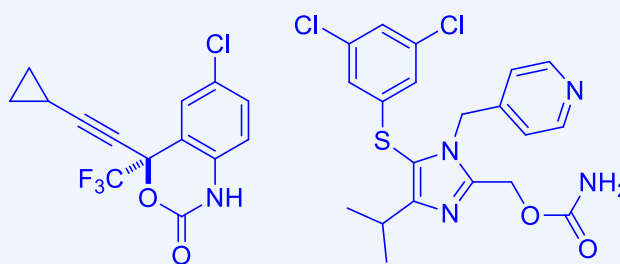
efavirenz (Sustiva, **31**)
BMS/Merck, 1998
NNRTI, wt IC_{50} = 14 nM

capravirine **32**
NNRTI
wt IC_{50} = 47 nM

molecular hybridation
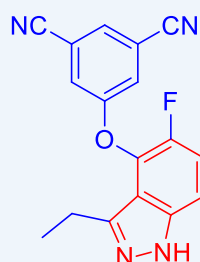
indazole **33**
NNRTI
wt IC_{50} = 25 nM
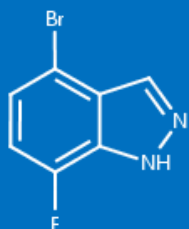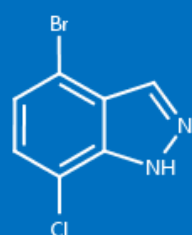
Bi-phenyl **34** was a reasonably potent bradykinin B1 (BB₁) receptor antagonist, but it suffered from a high permeability glycoprotein (Pgp) directional transporter ratio (it is considered high if the ratio is higher than 2.5). Scaffold hopping gave rise to a series of phenyl-indazoles as novel BB₁ receptor antagonists. Compound **35** in the series showed acceptable Pgp ratio and rat pharmacokinetic profile.[13]


bisphenyl **34**
hBK1 K_i = 1.5 nM
Pgp ratio = 4.1

phenyl-indazole **35**
hBK1 K_i = 0.12 nM
Pgp ratio = 2.3
P_{app} = 13
rat PK:
F% = 24
$t_{1/2}$ = 3.1 h
Cl = 2.5 mL/min/kg
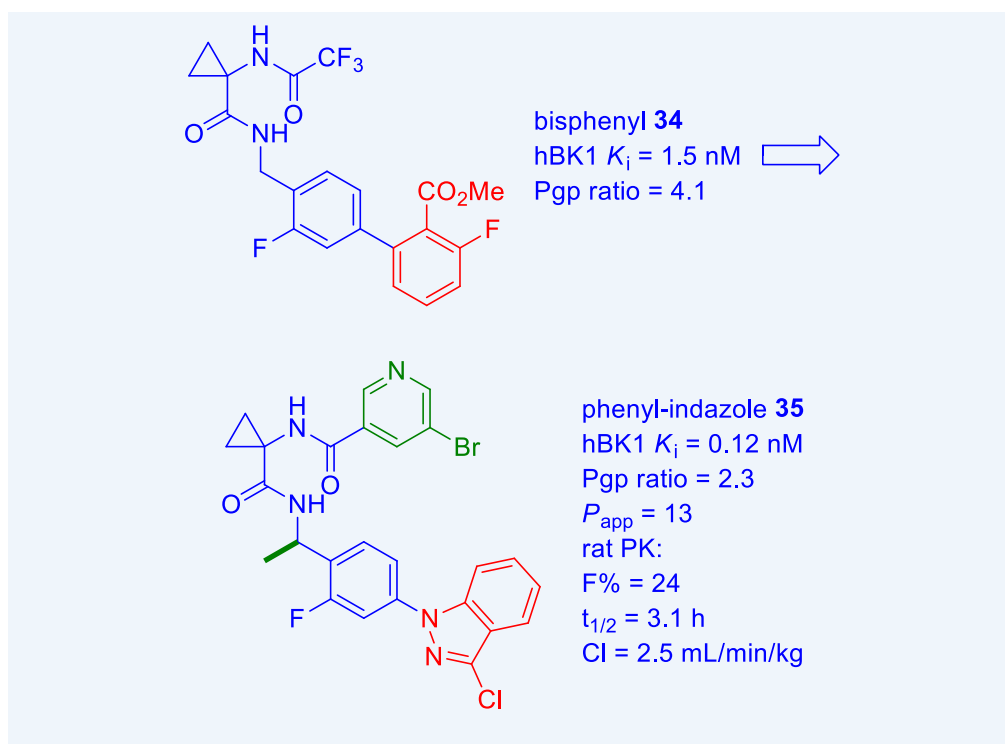
Bacterial DNA gyrase is a clinically validated target. Despite the excellent *Sa* GyrB binding potency, gyrase inhibitor pyrazolopyridone **36** does not show whole cell antibacterial activity. The lack of minimal inhibitory concentration (MIC) could be due to poor cell membrane penetration resulted from polar functional groups therefore, a low logD. In an effort to increase logD to improve cell penetration, a series of indazoles were prepared. Indazole **37**, in particular, possessed an excellent Gram-positive MIC profile in addition to retaining enzymatic activity.[14]

**PharmaBlock Products**
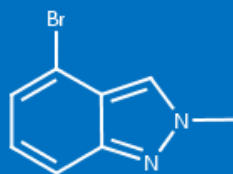
PB02008
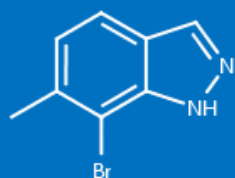
PBLJ0297
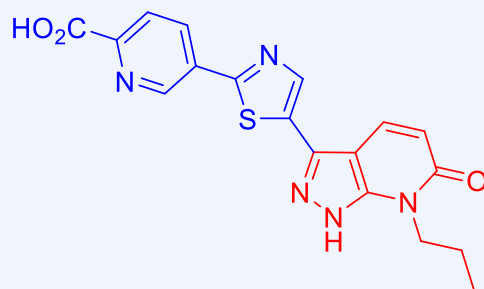
pyrazolopyridone **36**
S. au GyrB IC_{50} < 8 nM
S. au TopoIV IC_{50} = 56 nM
S. au MIC IC_{50} > 32 μg/mL
*S. pn* MIC IC_{50} = 0.06 μg/mL
logD (pH7.4) = –0.9
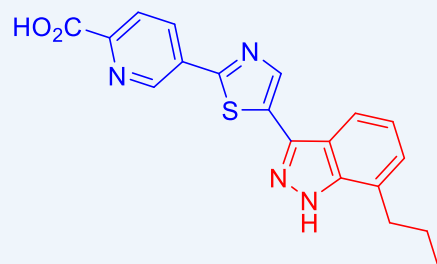
indazole **37**
S. au GyrB IC_{50} 10 nM
S. au TopoIV IC_{50} = 56 nM
S. au MIC IC_{50} = 0.06 μg/mL
S. pn MIC IC_{50} = 0.06 μg/mL
logD (pH7.4) = 1.7

Scaffold hopping has been a fruitful strategy to create novel intellectual properties (IP). For instance, pyrazole **38**, from the patent literature, was a G-protein-coupled receptor GPR120 agonist. AstraZeneca scientists speculated that rigidification of the ether side chain by connecting from oxygen to the pyrazole through installation of an indazole ring as in **39** would present a novel GPR120 agonists, and it did. Indazole **39** was potent for GPR120 with good selectivity against GPR40. It also had favorable pharmacokinetic profile and was tested efficacious in an oral glucose tolerance test (OGTT) mouse model.[15]
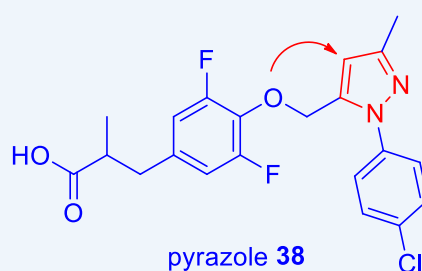
pyrazole **38**

scaffold

hopping
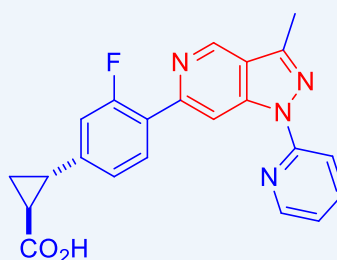
indazole **39**
h/mu GPR120
EC_{50} = 0.74/1.0 μM
mu GPR40
EC_{50} > 100 μM
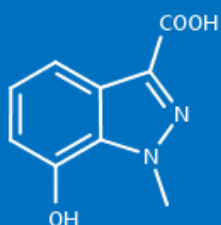
## Synthesis of Some Indazole-containing Drugs

In the synthesis of the nonsteroidal anti-inflammatory drug (NSAID) bendazac (**1**), benzylaniline **40** was used as its starting material. Nitrosylation was accomplished using nitrous acid. The resulting *N*-nitroso intermediate **41** was reduced with sodium thiosulfate to the corresponding hydrazine, which simultaneously cyclized to the indazolone **42**. Subsequent alkylation with methyl chloroacetate was followed by hydrolysis to deliver bendazac (**1**).[16]
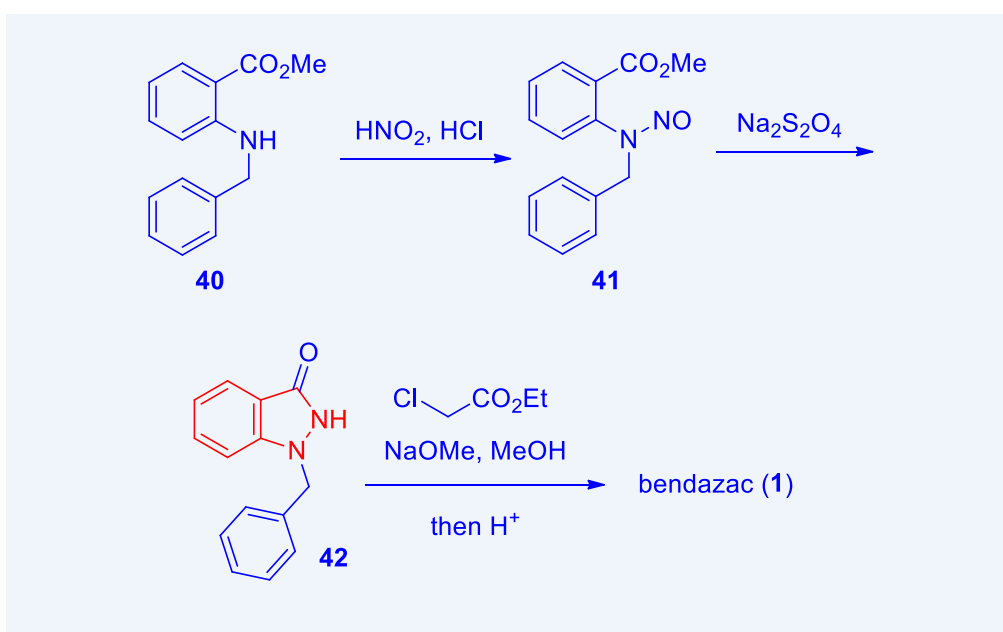

For the synthesis of Roche's granisetron (Kytril, **3**), 5-methoxyindazole (**43**) was protected as its SEM derivative **44**, which was then installed in the ethyl ester on the 3-position to give **45**. Switching the SEM group with a methyl group was accomplished by acidic hydrolysis to afford indazole **46** followed by methylation to produce **47**. Basic hydrolysis of **47** provided the 5-methoxy-1-methyl-indazole-3-carboxylic acid (**48**). Coupling **48** with the bicyclic amine **49** produced amide **50** and the methyl ether was converted into the benzyl ether. The end result was the benzyloxyl derivative of granisetron **51**.[17]

PharmaBlock Products
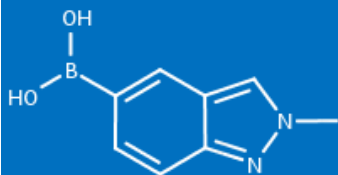
PB02004
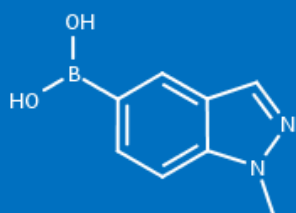
PB00500
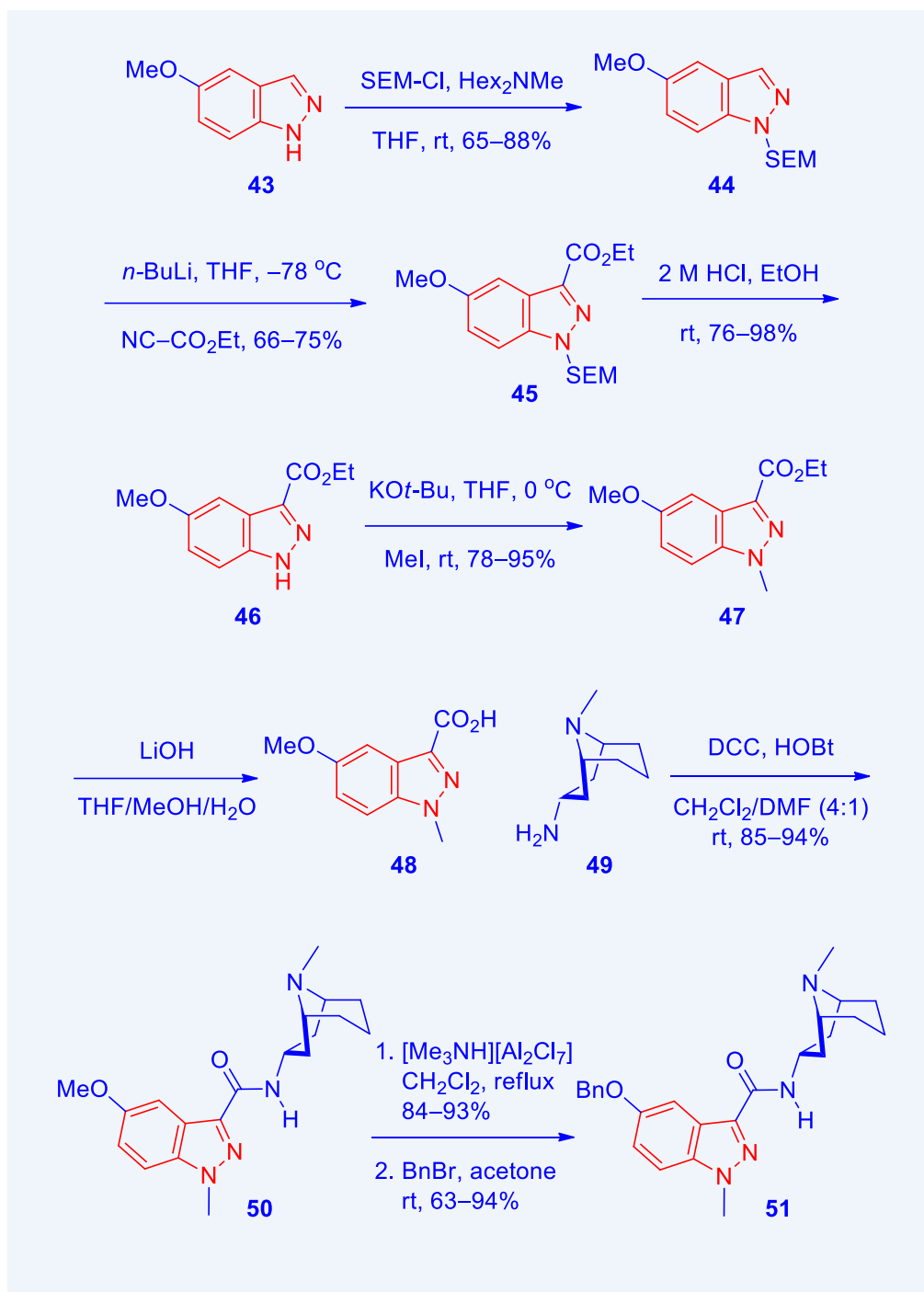
A synthesis of Merck's PARP inhibitor niraparib (Zejula, **6**) began with amidation of acid **52** with *t*-butylamine to make **53**. The C–N coupling between indazole **53** and phenyl bromide **54** assembled adduct **55**. Finally, double deprotection delivered niraparib (**6**).[18]
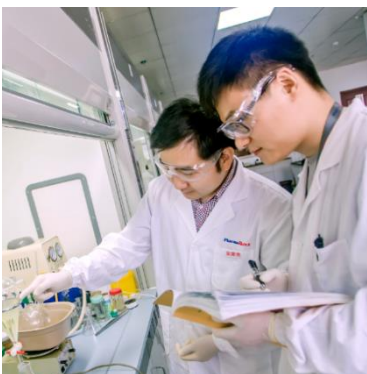
PharmaBlock is recognized for its outstanding capability in the design, synthesis, production and commercialization of novel building blocks for use throughout the drug R&D process.

- 80,000+ building blocks
- 16,000+ in stock in both USA and China
- 20,000+ supplied within two weeks
- 1,000+ SAR tool kits
- Novel building blocks designed upon daily monitoring on recent researches and patents
- Keep optimizing cost effective route for better price and sustainable supply
- Fast delivery of custom synthesis
- Enabling technologies of flow chemistry, biocatalysis, photochemistry, electrosynthesis, and fluorination, etc.
- Commercial production with GMP compliance
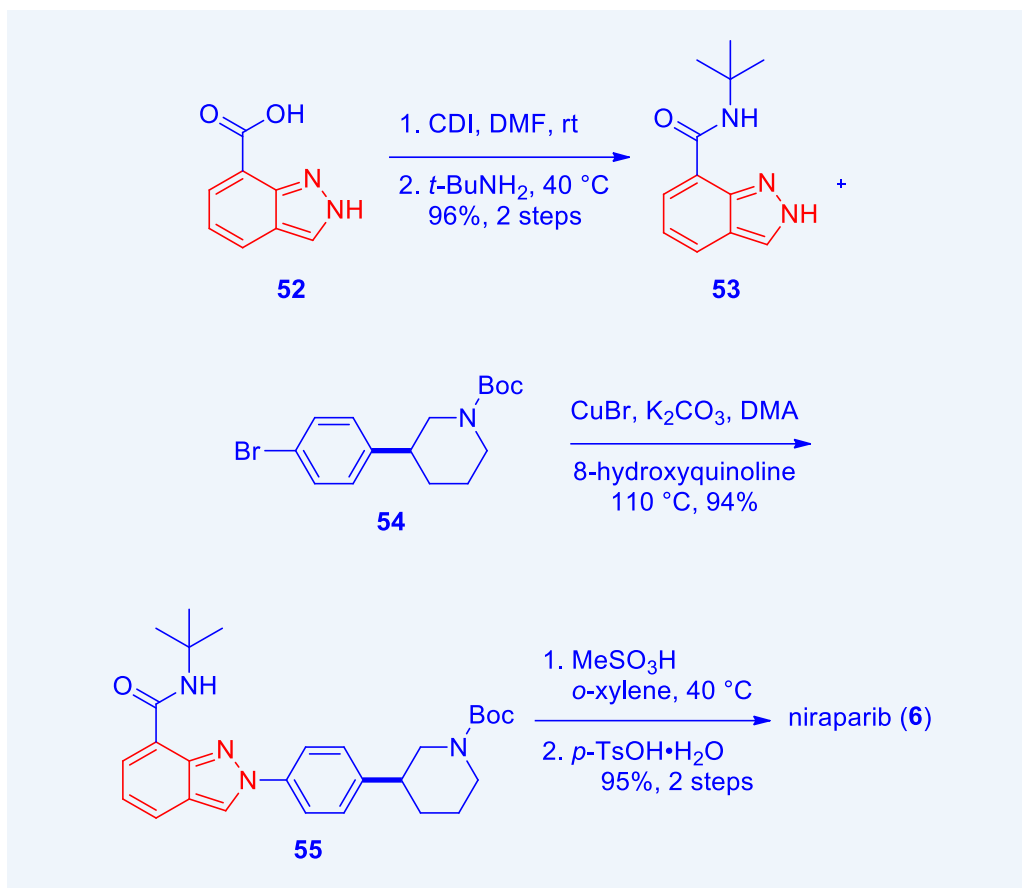
The synthesis Genentech's GDC-0941 (pictilisib, **13**) provides a good opportunity to appreciate indazole's isomerism during its preparation.

Diazotization of 3-bromo-2-methylaniline (**56**) was followed by basic cyclization to construct 4-chloroindazole (**57**). Carefully optimized conditions provided selective protection of **57** to give the desired isomer **58b** in 98% yield, which underwent a halogen−metal exchange followed by borylation to afford boronic acid **59**. Nickel-catalyzed coupling between **59** and benzotriazolyl-piperazine chloride **60** was proven to be superior to palladium catalysis to assemble adduct **61** since expensive scavenging residue palladium was circumvented. Acidic removal of the THP protection then delivered pictilisib (**13**).

Contact Us

PharmaBlock Sciences (Nanjing), Inc.
Tel: +86-400 025 5188
Email: sales@pharmablock.com

PharmaBlock (USA), Inc.
Tel (PA): 1-877 878 5226
Tel (CA): 1-267 649 7271
Email: salesusa@pharmablock.com
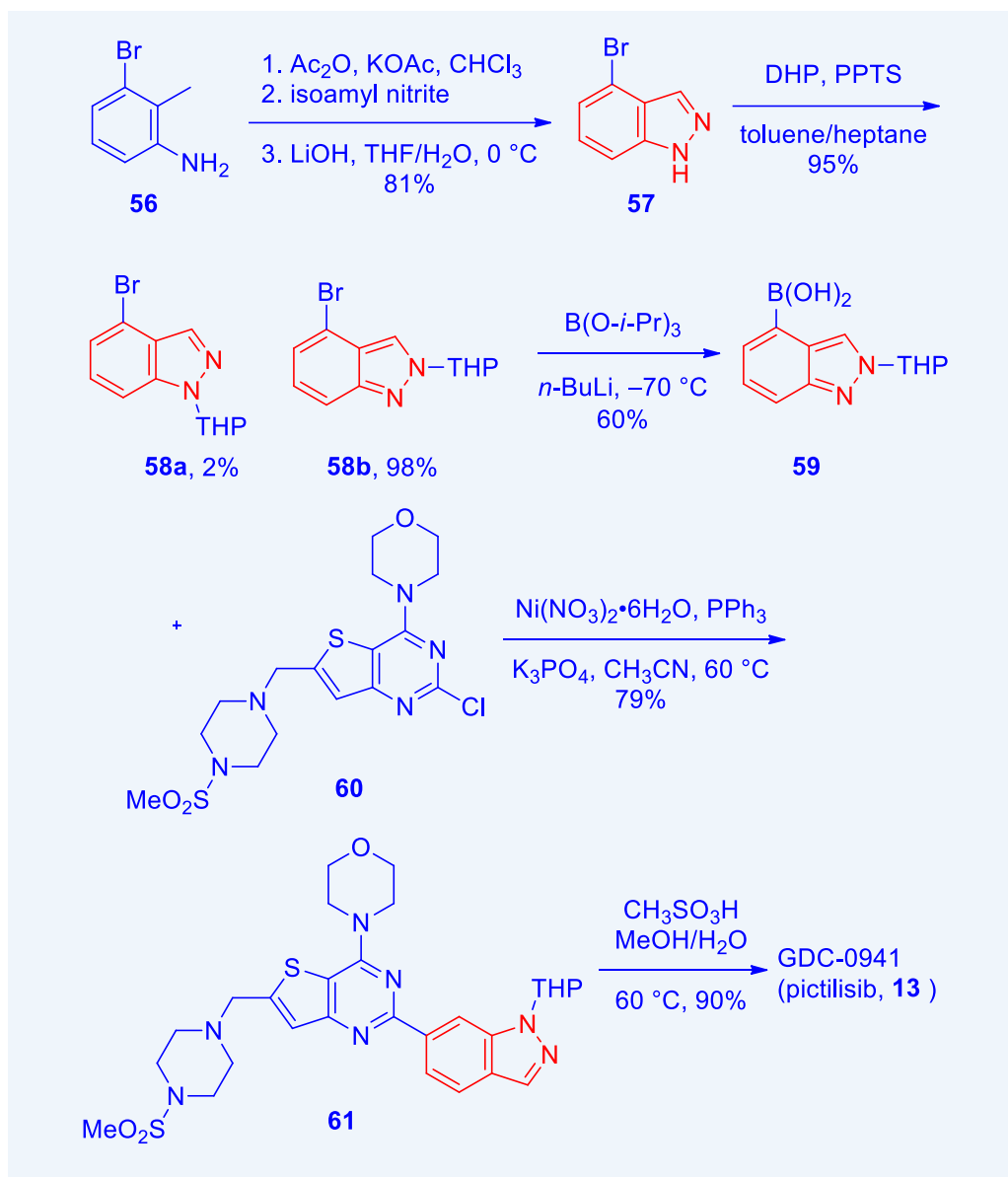
In summary, indazole is important in at least three major areas in medicinal chemistry. a. Indazole is a good bioisostere for phenol. Generally speaking, phenol's heterocyclic bioisosteres, including indazole, tend to be more lipophilic and less vulnerable to phase I and II metabolism in comparison to phenol. b. Indazole is a privileged fragment in FBDD. c. Indazole has proven to be a privileged scaffold in scaffold hopping exercises, especially for protein kinase inhibitors.

References

1. Wu, W.-L.; Burnett, D. A.; Spring, R.; Greenlee, W. J.; Smith, M.; Favreau, L.; Fawzi, A.; Zhang, H.; Lachowicz, J. E. *J. Med. Chem.* **2005,** *48*, 680–693.

2. Bamborough, P.; Angell, R. M.; Bhamra, I.; Brown, D.; Bull, J.; Christopher, J. A.; Cooper, A. W. J.; Fazal, L. H.; Giordano, I.; Hind, L.; et al. *Bioorg. Med. Chem. Lett.* **2007,** *17*, 4363–4368.

3. (a) Hayakawa, M.; Kaizawa, H.; Moritomo, H.; Koizumi, T.; Ohishi, T.; Okada, M.; Ohta, M.; Tsukamoto, S.-i.; Parker, P.; Workman, P.; et al. *Bioorg. Med. Chem. Lett.* **2006,** *14*, 6847–6858. (b) Folkes, A. J.; Ahmadi, K.; Alderton, W. K.; Alix, S.; Baker, S. J.; Box, G.; Chuckowree, I. S.; Clarke, P. A.; Depledge, P.; Eccles, S. A.; et al. *J. Med. Chem.* **2008,** *51*, 5522–5532.

4. Di Grandi, M. J.; Berger, D. M.; Hopper, D. W.; Zhang, C.; Dutia, M.; Dunnick, A. L.; Torres, N.; Levin, J. I.; Diamantidis, G.; Zapf, C. W.; et al. *Bioorg. Med. Chem. Lett.* **2009,** *19*, 6957–6961.

5. Antonysamy, S.; Hirst, G.; Park, F.; Sprengeler, P.; Stappenbeck, F.; Steensma, R.; Wilson, M.; Wong, M. *Bioorg. Med. Chem. Lett.* **2009,** *19*, 279–282.

6. Ritzén, A.; Sørensen, M. D.; Dack, K. N.; Greve, D. R.; Jerre, A.; Carnerup, M. A.; Rytved, K. A.; Bagger-Bahnsen, J. *ACS Med. Chem. Lett.* **2016,** *7*, 641–646.

7. Roughley, S. D.; Hubbard, R. E. *J. Med. Chem.* **2011,** *54*, 3989–4005.

8. Buchstaller, H.-P.; Eggenweiler, H.-M.; Sirrenberg, C.; Graedler, U.; Musil, D.; Hoppe, E.; Zimmermann, A.; Schwartz, H.; Maerz, J.; Bomke, J.; et al. *Bioorg. Med. Chem. Lett.* **2012,** *22*, 4396–4403.

9. Chang, C.-F.; Lin, W.-H.; Ke, Y.-Y.; Lin, Y.-S.; Wang, W.-C.; Chen, C.-H.; Kuo, P.-C.; Hsu, J. T. A.; Uang, B.-J.; Hsieh, H.-P. *Eur. J. Med. Chem.* **2016,** *124*, 186–199.

10. Wood, S. D.; Grant, W.; Adrados, I.; Choi, J. Y.; Alburger, J. M.; Duckett, D. R.; Roush, W. R. *ACS Med. Chem. Lett.* **2017,** *8*, 1258–1263.

11. (a) Engel, J.; Richters, A.; Getlik, M.; Tomassi, S.; Keul, M.; Termathe, M.; Lategahn, J.; Becker, C.; Mayer-Wrangowski, S.; Gruetter, C. et al. *J. Med. Chem.* **2015,** *58*, 6844–6863. (b) Tomassi, S.; Lategahn, J.; Engel, J.; Keul, M.; Tumbrink, H. L.; Ketzer, Ju.; Muehlenberg, T.; Baumann, M.; Schultz-Fademrecht, C.; Bauer, S.; et al. *J. Med. Chem.* **2017,** *60*, 2361–2372.

12. Jones, L. H.; Allan, G.; Barba, O.; Burt, C.; Corbau, R.; Dupont, T.; Knochel, T.; Irving, S.; Middleton, D. S.; Mowbray, C. E.; et al. *J. Med. Chem.* **2009,** *52*, 1219–1223.

13. Bodmer-Narkevitch, V.; Anthony, N. J.; Cofre, V.; Jolly, S. M.; Murphy, K. L.; Ransom, R. W.; Reiss, D. R.; Tang, C.; Prueksaritanont, T.; Pettibone, D. J.; et al. *Bioorg. Med. Chem. Lett.* **2010,** *20*, 7011–7014.

14. Zhang, J.; Yang, Q.; Romero, J. A. C.; Cross, J.; Wang, B.; Poutsiaka, K. M.; Epie, F.; Bevan, D.; Wu, Y.; Moy, T.; et al. *ACS Med. Chem. Lett.* **2015,** *6*, 1080–1085.

15. McCoull, W.; Bailey, A.; Barton, P.; Birch, A. M.; Brown, A. J. H.; Butler, H. S.; Boyd, S.; Butlin, R. J.; Chappell, B.; Clarkson, P.; et al. *J. Med. Chem.* **2017,** *60*, 3187–3197.

16. Shen, H.; Gou, S.; Shen, J.; Zhu, Y.; Zhang, Y.; Chen, X. *Bioorg. Med. Chem. Lett.* **2010,** *20*, 2115–2118.

17. (a) Bermudez, J.; Fake, C. S.; Joiner, G. F.; Joiner, K. A.; King, F. D.; Miner, W. D.; Sanger, G. J. *J. Med. Chem.* **1990,** *33,* 1924–1929. (b) Vernekar, S. K. V.; Hallaq, H. Y.; Clarkson, G.; Thompson, A. J.; Silvestri, L.; Lummis, S. C. R.; Lockner, M. *J. Med. Chem.* **2010,** *53,* 2324–2328.

18. Hughes, D. L. *Org. Process Res. Dev.* **2017,** *21,* 1227–1244.

19. Tian, Q.; Cheng, Z.; Yajima, H. M.; Savage, S. J.; Green, K. L.; Humphries, T.; Reynolds, M. E.; Babu, S.; Gosselin, F.; Askin, D.; et al. *Org. Process Res. Dev.* **2013,** *17,* 97–107.